Nano Energy 92 (2022) 106786

Contents lists available at ScienceDirect

Nano Energy

journal homepage: www.elsevier.com/locate/nanoen

Human joint enabled flexible self-sustainable sweat sensors

Hu Li [a,b,1], Tianrui Chang [a,1], Yansong Gai [c,1], Kui Liang [d,1], Yanli Jiao [b], Dengfeng Li [b,f], Xinran Jiang [a], Yang Wang [a], Xingcan Huang [b], Han Wu [a], Yiming Liu [b], Jian Li [d], Yiming Bai [d], Kai Geng [d], Nianrong Zhang [g], Hua Meng [g], Dongsheng Huang [d,*], Zhou Li [c,*], Xinge Yu [b,f,**], Lingqian Chang [a,e,***]

[a] Key Laboratory of Biomechanics and Mechanobiology, Ministry of Education, Beijing Advanced Innovation Center for Biomedical Engineering, School of Biological Science and Medical Engineering, Beihang University, Beijing, 100083, China
[b] Department of Biomedical Engineering, City University of Hong Kong, Hong Kong, China
[c] Beijing Institute of Nanoenergy and Nanosystems, Chinese Academy of Science, Beijing 101400, China
[d] BOE Technology Group Co., Ltd, China
[e] School of Biomedical Engineering, Research and Engineering Center of Biomedical Materials, Anhui Medical University, Hefei 230032, China
[f] Hong Kong Center for Cerebra-Cardiovascular Health Engineering, Hong Kong Science Park, New Territories, Hong Kong, China
[g] General Surgery Department & Obesity and Metabolic Disease Center, China-Japan Friendship Hospital, Beijing 100029, China

ARTICLE INFO

Keywords:
Sweat sensor
Human joints
Self-sustainable electronics
Wireless signal transmission
Flexible and wearable electronics

ABSTRACT

Flexible and wearable electronics have presented a wide range of advantages to non-invasive real-time human health monitoring. However, its remarkable energy consumption during continuous and long-time operation brings essential, practical challenges, which lead to growing recognition of exploring new and efficient energy strategies for wearables. Here, inspired by human joints as a biomechanical energy source that shows an ideal option for sustainable powers, we design a battery-free sweat sensing system integrated with sweat resistant self-sustainable energy supply and wireless communication interface, where piezoelectric nanogenerators (PENGs) efficiently converting biomechanical energy from freely movable joints (finger, cubital fossa and popliteal space) into electricity serving as the self-powering module. Physiological relevant parameters in sweat, including Na+, K+ and pH, are sensed and wirelessly transmitted to the user interface via Bluetooth communication. This system shows a paradigm of wearable electronics driven by human joints that demonstrated efficient self-sustainable energy supply and multiplexed physiological detection.

1. Introduction

Human in extensive exercise generates large amounts of sweat that contains a wide variety of secretions, including hormones, metabolites, electrolytes, and amino acids. Most of these substances play important roles in determining or indicating health conditions [1–4]. For example, concentrations of Na^+ and K^+ in sweat, accompanied by pH change, are three important biochemical markers to provide valuable reference to medical diagnosis (e.g., cystic fibrosis, dermatosis, diabetes) [5,6]. Conventional sweat sensors at early stage adopted rigid substrates that often caused discomfortability issue (e.g., oppressing sensation) due to the low conformability of devices to skin surface [7,8]. The emerging thin, soft, flexible and wearable electronics have revolutionized traditional medical equipment, as the soft sensor patches replace rigid bulky devices to a certain extent, making biochemical markers monitoring in sweat more convenient, comfortable and user friendly [9–14].

The power sources of sweat sensors typically rely on bulky rigid batteries in the integrated circuit for data processing and signal transmission [15]. Flexible batteries have been developed to solve this problem to make the whole device easier and more conformal to skin surface. Another good strategy is adopting small size battery cells to power the circuits [16,17]. Albeit noticeable advantages, these batteries

* Corresponding authors.
** Corresponding author at: Department of Biomedical Engineering, City University of Hong Kong, Hong Kong, China.
*** Corresponding author at: Key Laboratory of Biomechanics and Mechanobiology, Ministry of Education, Beijing Advanced Innovation Center for Biomedical Engineering, School of Biological Science and Medical Engineering, Beihang University, Beijing, 100083, China.
E-mail addresses: huangdongsheng@boe.com.cn (D. Huang), zli@binn.cas.cn (Z. Li), xingeyu@cityu.edu.hk (X. Yu), lingqianchang@buaa.edu.cn (L. Chang).
[1] These authors contributed equally to this work.

https://doi.org/10.1016/j.nanoen.2021.106786
Received 14 October 2021; Received in revised form 23 November 2021; Accepted 24 November 2021
Available online 29 November 2021

meet limitations of frequent charge and replacement, or even the risk of self-explosion. Compared with batteries, renewable energy strategies (e.g., solar energy or biomechanical energy) [18–21] provide sustainable power management strategies, exhibiting great potential for powering novel flexible and wearable electronic devices in the future.

Among a wide range of applicable renewable energy harvesting approaches is the biomechanical energy in human body that are generated during body movements, such as running, riding, lifting dumbbell and even fist clenching [22]. Meanwhile, most exercises are accompanied with extensive joint bending and sweating. To harvest and convert mechanical energy, the recent advance in triboelectric nanogenerator (TENG) [23–28] and piezoelectric nanogenerator (PENG) [29–36] shows promising application scenarios to a wide range of fields in converting mechanical energy. Extensive activities from body motions often create watery environment (e.g., sweating and biofluid), TENGs therein is hindered by water screening effect due to their intrinsic working principle, i.e. the coupling of triboelectric and inductive effects [21,37–40], which manifests as a remarkable reduction in its electric output and energy conversion efficiency. In contrast, PENG based devices are competent in such environments because the piezoelectric effect relies on electric dipoles migration inside the materials [41,42]. Ever since the invention of PENGs, scientists have taken efforts to apply the PENG in biomedical engineering. For example, cardiac pacemakers [43], blood pressure sensors [44], cardiac sensor [45], pulse sensors [46], deep brain stimulation [47]. These achievements fully proved that PENG as energy harvester can not only serve as power sources, but also active sensors and electric stimulators in biomedical fields.

Inspired by human joints, we utilized PENG fixed on joints to trigger piezoelectric effect and convert biomechanical energy into electricity. Combining these strengths, it would be significant to develop sweat resistant energy harvesters based on piezoelectric technique to convert joint bending into electricity, and at the same time to power electronics for the motion generated sweat sensing. Many 2D materials (e.g., PANI/CNT [48], MoO_3 [49], MXene [50,51]) can be well used in sensing devices because of their large specific area and high density of reactive sites. However, these materials are improper for PENG due to the lack of piezoelectric property and device integration. Among piezoelectric materials (see Table S1 and Table S2), polyvinylidene fluoride (PVDF) is preferred in wearable electronics due to its intrinsic piezoelectric ability, film-forming property and good flexibility.

In this work, we reported integration strategies of a human-joint-enabled flexible and wearable self-sustainable sweat sensor patch (FWS^4P) based on PENG. The FWS^4P consists of a piezoelectric nanogenerator as the self-sustainable power source, a low-power integrated circuit on flexible printed circuit board (PCB) for power management and signal processing, a flexible microfluidic patch for sweat collection, and a sweat sensor array for multiplexed biomarker analysis (i.e., $[Na^+]$, $[K^+]$ and pH). The preparation technology of industrial-level flexible PCB is comparable to that of traditional rigid PCB, ensuring its high reliability and mass production capability. Flexible multilayered PENG is ideal to attach onto human joints, to effectively harvest the biomechanical energy, and providing electricity for skin-interfaced wearable electronics. This design demonstrates an important attempt to construct battery-free, piezoelectricity-based flexible and wearable self-

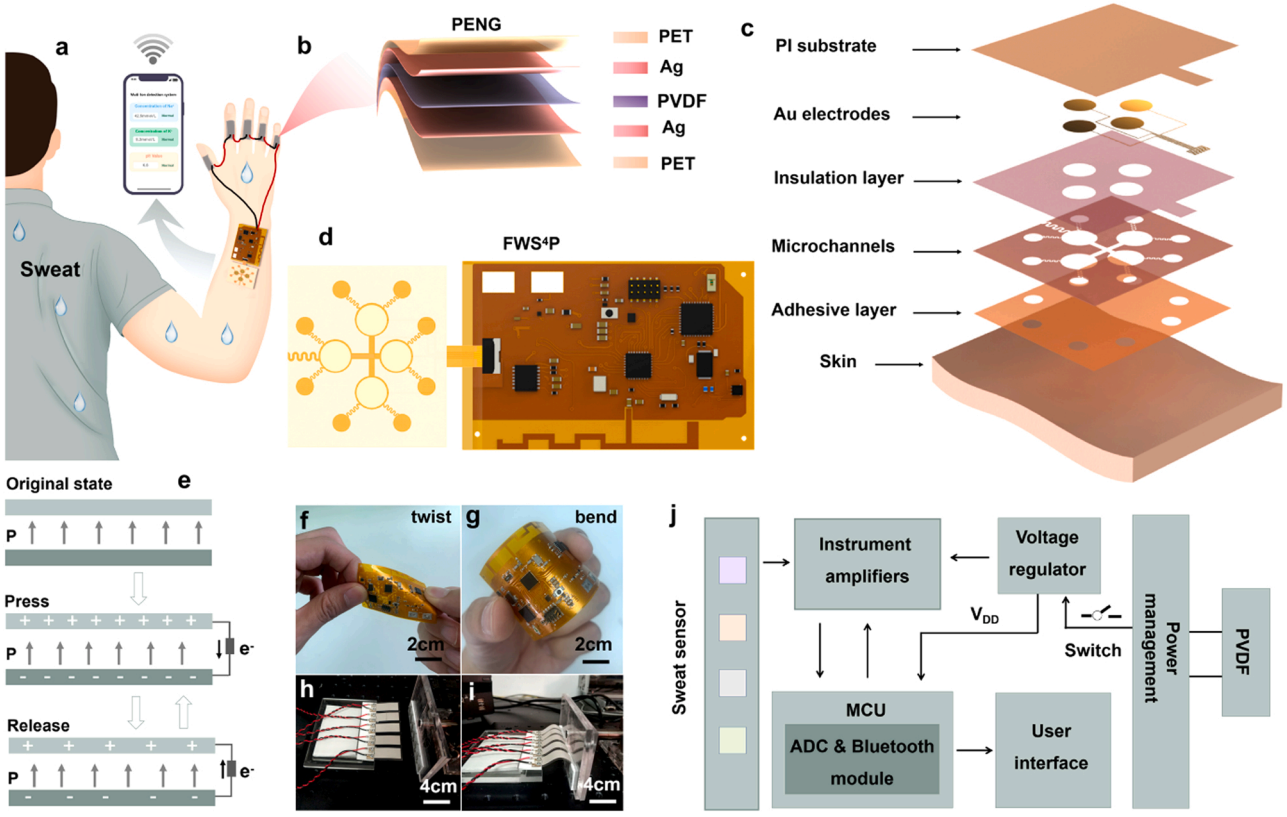

Fig. 1. Concept graph and structure diagram of FWS^4P. (a) Schematic diagram of finger-joint-enabled FWS^4P with wireless signal transmission to a user interface. PENG converts mechanical energy of finger joints into electricity and power the flexible circuit. Physiological information of sweat was detected by the sensor patch, processed by flexible circuit and transmitted to user interface. (b) Diagram of PENG with a layer-by-layer structure. PET, Ag and PVDF serve as supporting substrate, electrode layer and piezoelectric layer, respectively. (c) Structure diagram of sweat sensor patch attached to human skin. It consisted of five layers from up to down, including PI substrate, Au electrodes, insulation layer, microchannels and adhesive layer. Au electrodes include one reference electrode and three working electrodes. Microchannels have eight inlets, four chambers and one outlet. (d) Diagram of integrated flexible and wearable sweat sensor patch. (e) Working mechanism of PENG when suffered from joint bending. Picture of twist (f) and bending (g) of the flexible printed circuit board. Picture of bending test of PENG stripe by a linear motor (h-i), PENG size is 4 cm × 1.5 cm. (j) Block diagram of the whole system showing power management, signal processing and wireless transmission to user interface.

sustainable sweat sensor patch. Further, it establishes a versatile platform for eco-friendly and sustainable wearable electronics.

2. Results and discussion

As shown in Fig. 1a, the PENG strips are taped onto the back of fingers, covering all five proximal interphalangeal joints, and the FWS^{4}P is attached on the back of the forearm. The strips convert the biomechanical energy harvested during frequent fist clenching into electricity, which is stored in the capacitor on the PCB, then used to power the adjacent sweat sensor. The sweat biomarker information ([Na^+], [K^+], pH) is wirelessly transmitted to a user's smartphone via the Bluetooth module in circuit. The PENG has a palindrome 5-layer structure (Fig. 1b), with a polyethylene terephthalate (PET) substrate, a silver (Ag) back electrode and a polyvinylidene fluoride (PVDF) piezoelectric film from the outmost layer inwards. Each PENG strip measures 4 cm × 1.5 cm × 100 μm and weighs 0.6058 g (Fig. S1). The thin, light and flexible features ensure its good attachment on human joints. The sweat sensor consists of five layers, including a flexible polyimide (PI) substrate layer, a gold (Au) electrode (three working electrodes and one reference electrode) layer, an isolation layer (SU-8 photoresist), a microchannels layer (SU-8 photoresist) to collect sweat (Fig. S2), and an adhesive layer (medical tape) to attach the sensor to skin surface like a patch (Fig. 1c and Fig. S3). The ends of Au electrodes are connected to the flexible circuit through a narrow bridge as a demountable design (Fig. 1d). The circuit shows excellent flexibility when the device is twisted or bent (Fig. 1 f and g). Various electronic units are integrated in the circuit to achieve signal collection, processing and transmission, including power management, voltage regulator, instrument amplifiers, MCUs, ADC ports and Bluetooth modules as illustrated by Fig. 1j. The power management unit controls electric flux into the FWS^{4}P, i.e. it close the circuit and releases the electricity when voltage of its built-in capacitor reached the threshold value. The working principle of PENG was stated as follows: In the original state where the PENG strips are laid flat, the electric dipoles in the PVDF are align vertically between the top and the bottom electrodes (Fig. 1e); When PVDF strips undergo frequently bending (Fig. 1 h and i), the polarization charge density in the PVDF increases and generates an electric field, which compels electrons

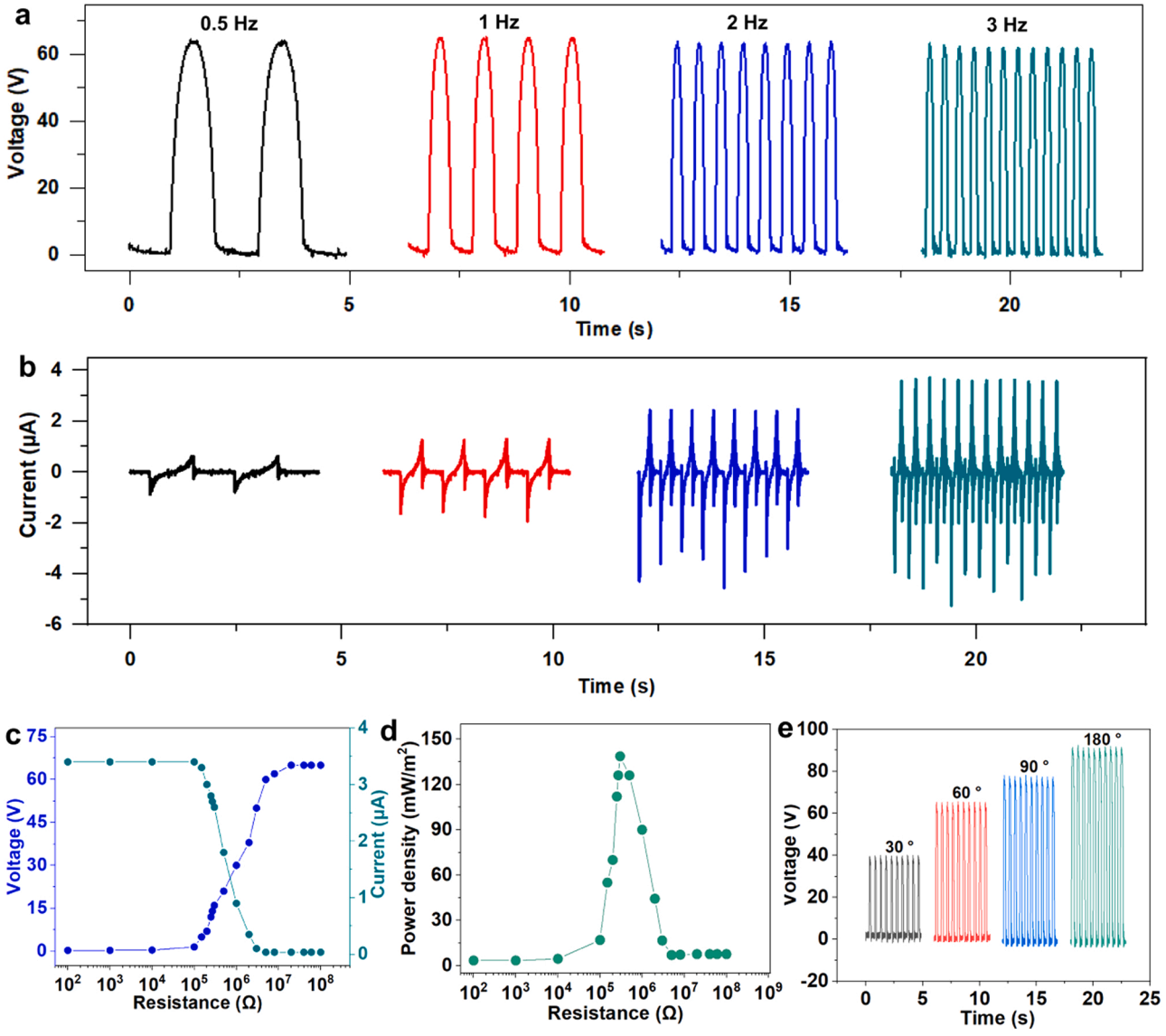

Fig. 2. Electrical characterization of a single PENG stripe. (a) Voltage variation and (b) Current variation of a single PENG under different frequencies from 0.5 Hz to 3 Hz. The voltage is around 65 V; The current increases with frequency increases. (c) Relationship of output voltage and current versus external loading resistance. (d) Relationship of power density versus loading resistance. The maximum power density reached to 140 mW/m^2. (e) Variation of output voltage at different bending angles from 30° to 180°.

to flow from the top electrode to the bottom electrode (Fig. 1e, press); When the external force disappears and the strips gradually recovers from deformation, electrons flow back in opposite direction (Fig. 1e, release).[52] Periodic bending and recovery of PVDF bring periodic current through the external circuit.

To characterize the electrical performance of a single PENG strip, we tested its open-circuit voltage (V_{oc}), short-circuit current (I_{sc}) and transferred charge at different frequencies of its bending cycle from 0.5 Hz to 3 Hz. The bending angle was fixed at 60°. The V_{oc} remained stable around 65 V (Fig. 2a) despite the change in frequency. The I_{sc} increased from 1 μA to 5 μA as frequency increases because a high frequency usually means a high flow rate of electron, which generates a higher output current (Fig. 2b). Meanwhile, the amount of transferred electrons was also measured stably around 100 nC for each bending circle (Fig. S4). A peak power density of a single PENG strip was observed at 140 mW/m^2 as V_{oc} and I_{sc} were recorded with a series of loading resistance from 100 Ω to 10^8 Ω (Fig. 2c and d). Additionally, the V_{oc} increased from 40 V to 90 V as the bending angle increased from 30° to 180° (Fig. 2e), which could be mainly attributed to the increased polarization charge density at a larger bending angle. The electric performance test of single PENG demonstrated outstanding ability for harvesting mechanical energy, it also provides strategy for electrical connection (in series or parallel) of multiple energy harvesters.

When the PENG strips are attached to fingers, they may be connected in series or in parallel. Compared with in series connection, in parallel connection should be able to provide a much higher current than in series connection, leading to a faster charging rate of the capacitor. Next, we connected fifteen PENG strips in parallel with three on each fingers. At a bending frequency of 3 Hz, the output voltage was about 93 V (Fig. 3a), and the output current reached to 48 μA (Fig. 3b).

With the same number of PENG strips connected in series, an output voltage of about 550 V and a current of 3.5 μA (Fig. S5) conclude that in parallel connection is indeed a more suitable strategy in that it allows for faster charging of the capacitor (Fig. S6). Considering that triboelectricity is usually remarkably reduced by water screening effect in damp environments, we tested the electric performance of PENG energy harvester in simulated sweat. PENG strips demonstrated stable electric output at 95 V (Fig. 3c), ensuring their unhindered application in pair with the FWS^{4}P. Five types of capacitors were charged with fifteen PENG strips connected in parallel after rectifying the converted electricity to evaluate PENG's charging performance. It took a few seconds for the single 100 μF capacitor to be charged to 3.7 V, which is higher than the threshold voltage (3.2 V) required to turn on the circuit. Charging time for the other larger capacitors (470 μF, 1000 μF, 5 * 470 μF in parallel and 5 * 1000 μF in parallel) were 3.5 min, 6.2 min, 20.7 min and 35 min, respectively (Fig. 3d). Among them, the capacitor

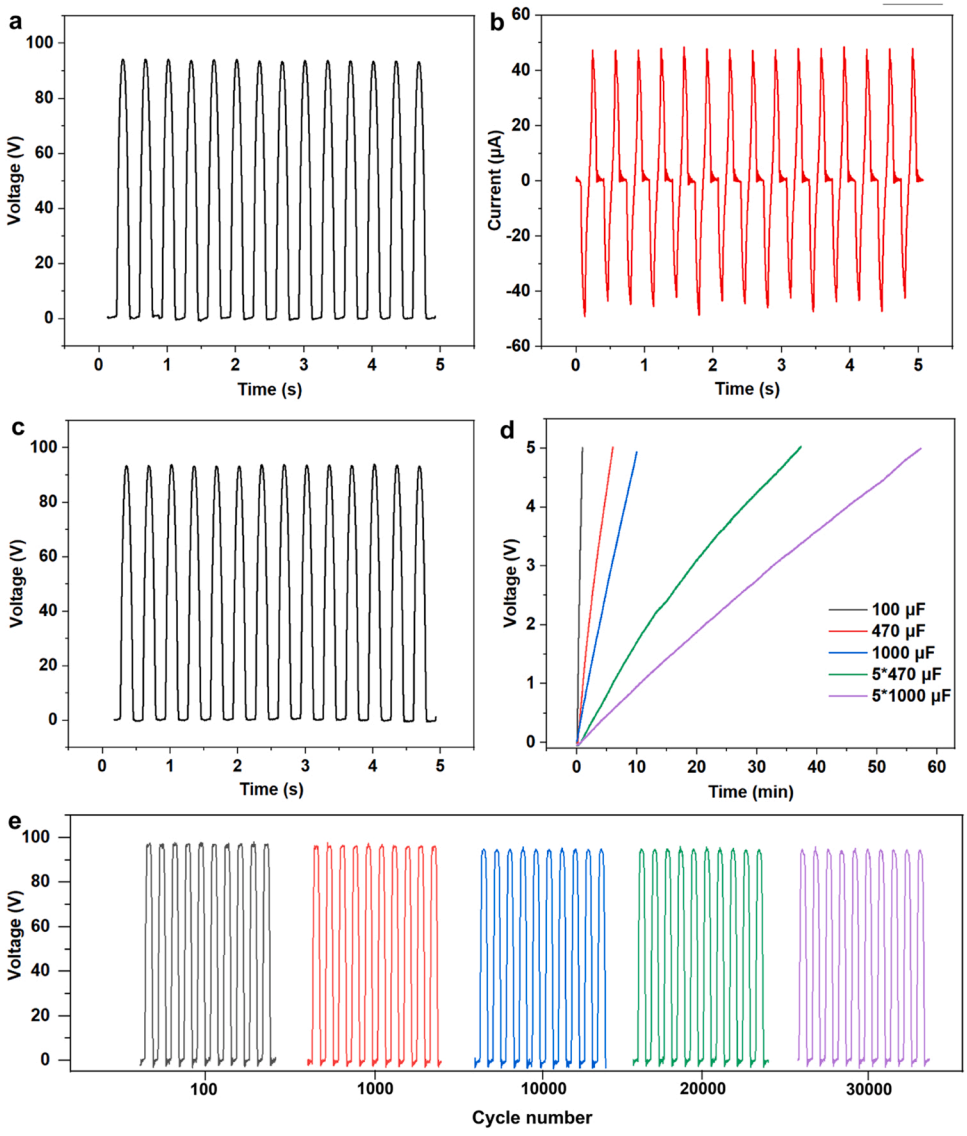

Fig. 3. Parallel connection performance and bending performance of fifteen PENG stripes. (a) Output voltage and (b) output current of fifteen PENGs in parallel connection in air. (c) Output voltage of fifteen PENGs in parallel connection with water on its surface. (d) Charging curves of different capacitors with fifteen PENGs in parallel connection. (e) Cycling performance of a single PENG stripe for 30,000 bending test. The measurement was carried out using a linear motor. All the bending angle in this part is 180°.

of 5 * 1000 μF capacitors in parallel was used to power the sweat sensor system in the following experiments. To test fatigue resistance of the nanogenerators to bending, we conducted a 30, 000 cycle bending test on one PENG strip. The output voltage remained stable around 97 V; no significant decay was observed throughout the bending test.

The design and performance of the sweat sensor patch are illustrated in Fig. 4. The naked Au electrodes in the sweat sensor were further processed to carry out their composition analysis duty. To detect specific ions, selective membranes were mounted onto the electrodes with a PEDOT:NaPSS layer in between. Meanwhile, it can minimize the potential drift serving as an ion-electron transducer. Fig. S7 illustrates the layered structure and working mechanism of the ion-selective sensors. The measurement of ion concentration was facilitated via a Na^+ ionophore X containing membrane on the Na^+ ion-selective electrode (ISE) and a valinomycin-containing membrane on the K^+ ISE. A selectivity test was carried out to ensure that each sensor was able to specifically detect corresponding ions (Fig. S8). The response curve of the Na^+ ISE showed outstanding specificity to Na^+, and no obvious changes while Ca^{2+} and K^+ were added as interference. Similar results were observed for the K^+ ISE, where Ca^{2+} and Na^+ were added as

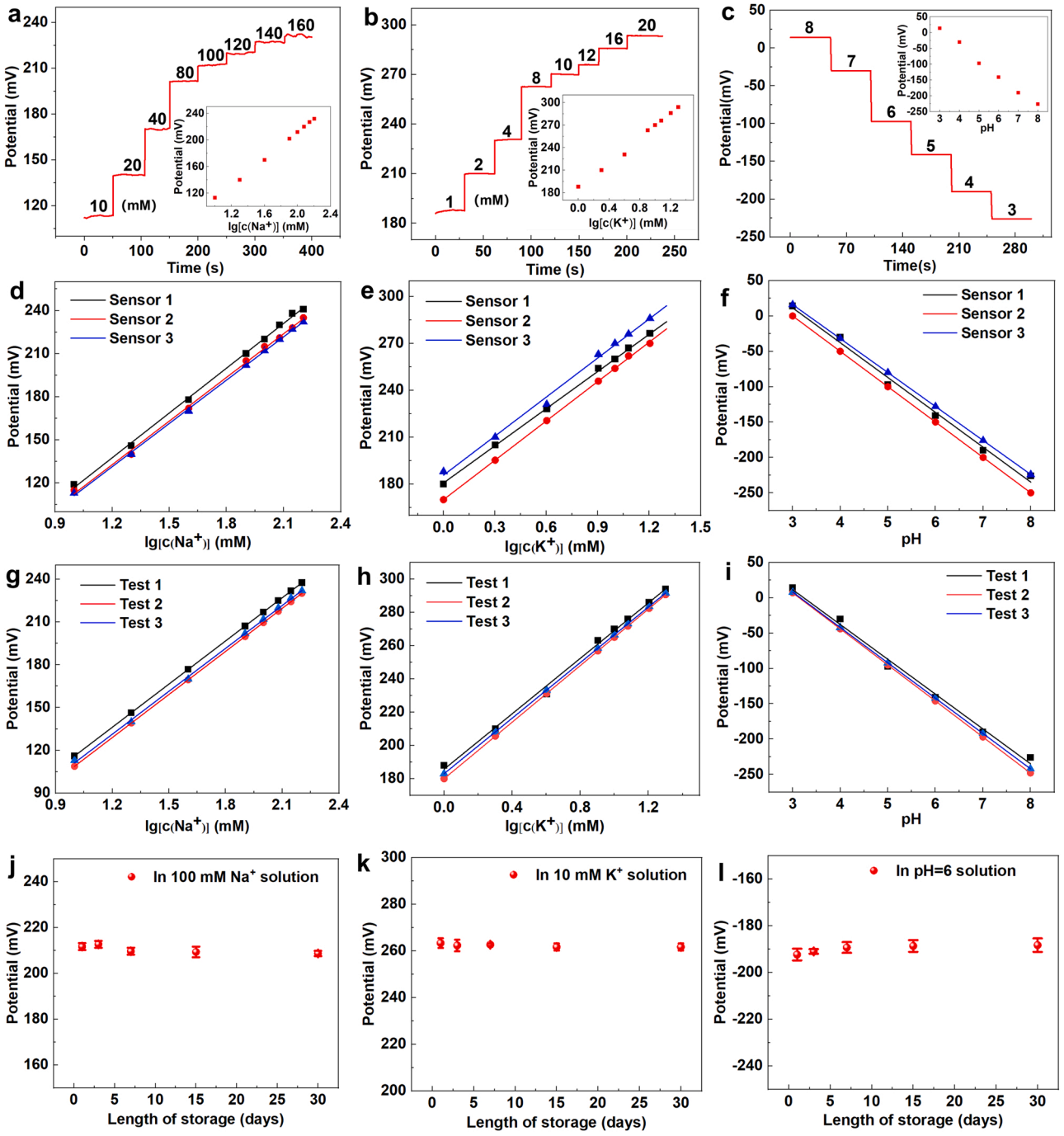

Fig. 4. Sensing property of sweat sensor patch in room temperature. (a-c) Open-circuit potential response of a Na^+ sensor in NaCl solution with concentrations from 10 mM to 160 mM (a), a K^+ sensor in KCl solution with concentrations from 1 mM to 20 mM (b), and a pH sensor in McIlvaine's buffers with pH values from 3 to 8 (c). (d-f) Consistency valuation between different sensors of Na^+ (d), K^+ (e) and pH (f). The sensitivity variation is lower than 5%. (g-i) Repeatability valuation between different sensors of Na^+ (g), K^+ (h) and pH (i). The sensitivity variation is lower than 5%. (j-l) Stability valuation of Na^+ sensor (j), K^+ sensor (k) and pH sensor (l) for 30 days.

interference. For pH analysis, the pH ISE was modified by mounting a $HAuCl_4$ layer and a polyaniline (PANI) layer, respectively, on the Au electrode to achieve H^+ sensitivity.

To maintain steady potential responses of the sensors, polyvinyl butyral (PVB) was adopted and coated on Ag/AgCl reference electrode. These ISEs show ideal performance across the entire spectrum of physiologically relevant conditions, i.e. Na^+ concentrations of 10–200 mM, K^+ concentrations of 1–20 mM and pH levels of 3–8. Representative voltage responses of Na^+ and K^+ and pH ISEs show near-Nernstian sensitivities of 65.72, 52.83 and 55.44 mV per decade concentration,

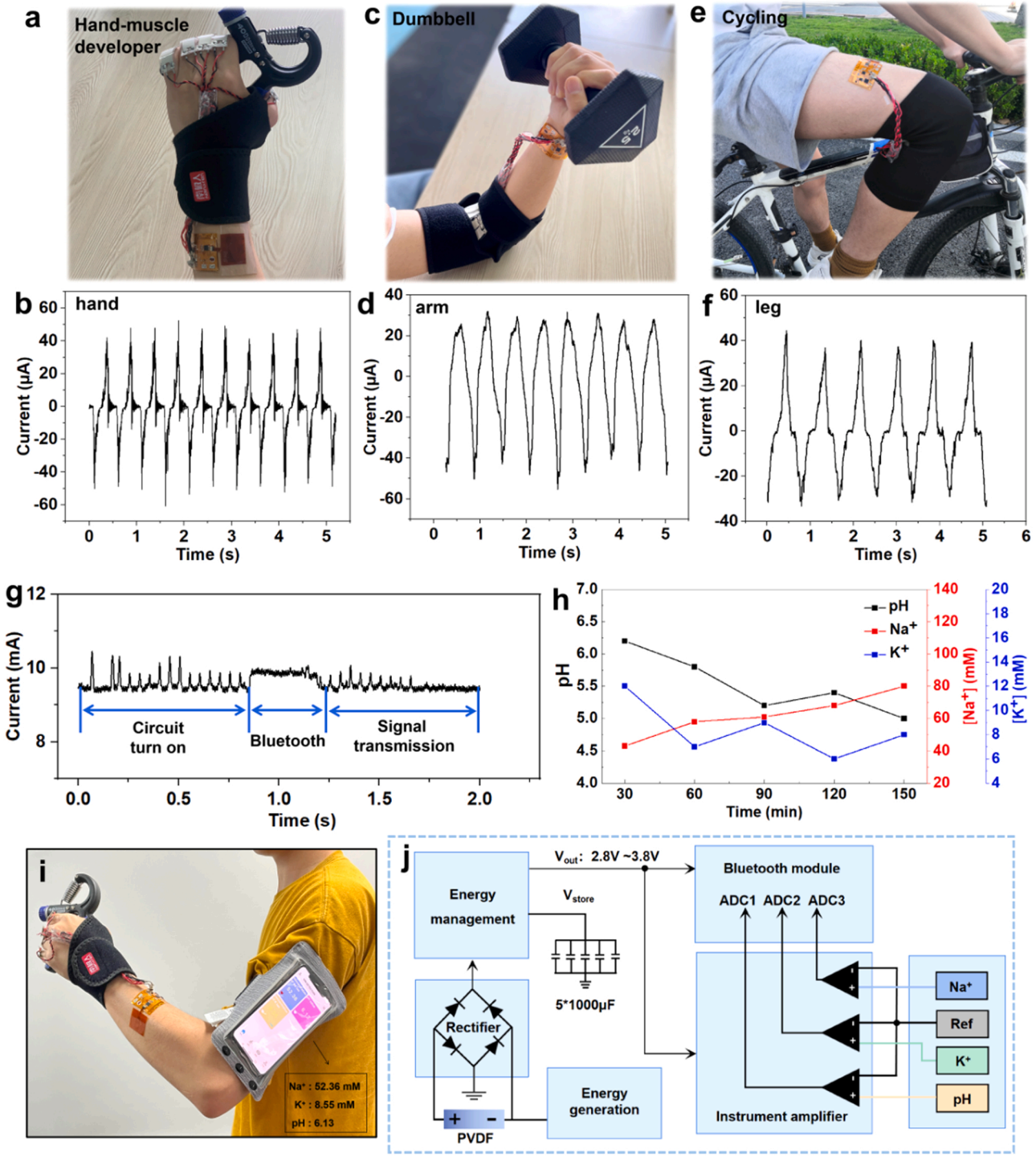

Fig. 5. Application demonstration of FWS^{4}P attached on different human joints, e.g., finger joint, arm joint and leg joint. (a) Hand-enabled energy harvesting, and powering sweat sensor by gripping a hand-muscle developer. PENG converted mechanical energy of clenching fist into electricity. (b) Output current by clenching fist with a hand-muscle developer. (c) Cubital-fossa-enabled energy harvesting, and powering sweat sensor by dumbbell curling. PENG converted mechanical energy of bending arm into electricity. (d) Output current by training arm muscle with a dumbbell, PENGs are attached to cubital fossa. (e) Popliteal-space-enabled energy harvesting, and powering sweat sensor by riding a bike. PENG converted mechanical energy of leg bending into electricity. (f) Output current by training leg muscle with biking, PENGs are attached to popliteal space. (g) Variation of circuit current during sweat sensor operation. (h) Wireless monitering of Na^+, K^+ and pH, powered by biking for 150 min, five data points were collected during the exercise. (i) Photograph of hand-enabled sensing of pH, Na^+ and K^+, after clenching fist for 30 min, the circuit was turned on. (j) Module diagram of practically operating the self-sustainable sweat sensor.

respectively, at room temperature (Fig. 4a, b and c). Multiple sensors of each ion type were fabricated and three of each were picked to demonstrate sensor consistency. For each ion type, the triplicate sensors show nearly identical absolute potentials with a low variation (< 5%) in sensitivity (Fig. 4d, e and f). Repeatability of the sensors is demonstrated in Fig. 4g, h and i, each sensor has been tested for three times, and the results show low variation (< 5%) in sensitivity. The sensor stability was tested over one month, in conditions that more closely mimic human sweat during exercises. Measurement results with fluctuation less than 5% of each sensor indicate good stability for long-term use (Fig. 4j, k and l).

A microfluidic channel is mounted onto the sweat sensor patch before the final adhesive layer for controlled and automatic on-body sweat sampling (Fig. S2). For sweat sensors on skin, inlets are designed to collect sweat into chamber by capillary force of microfluidic channel [53,54], one to four inlets for each chamber are reported in literature based on their requirements [55–57]. In general, more inlets usually mean a faster sweat collection rate to fill the chamber. Considering that sweat is not evenly distributed on skin, more than one inlet is preferred to achieve a faster sweat collection. On the other hand, take into account the limited area of the sensor patch and overall esthetic appearance, two inlets for each chamber (eight inlets in total) is adopted in our work. The sweat collected gets analyzed by the ISEs in the reaction chamber. The waste solution after analysis exits from the outlet. The flexibility of the microfluidic sensor patch allows it to adhere conformally to human skin, indicating its applicability for a variety of sports scenarios. When adhere the sweat sensor patch onto skin or peel it off from skin, it is inevitable to cause bending and deformation to the sensor patch. To prove the stability of sensor patch can resist the bending and deformation, we tested its performance with 200 cycles of bending, which showed good stability before and after deformation (see Fig. S9). Besides, the long-term stability when detect ions was also tested for 6 h (see Fig. S10), which proved the sweat sensor is capable of detecting sweat in long-term sports scenes.

Next, the FWS^{4}P was put to test in daily exercise scenarios. Besides finger joints, the PENG strips can be fixed onto any joints (e.g., elbows, knees) to harvest the biomechanical energy generated through joint bending, and power the sweat sensor patch. Fig. 5 demonstrates the application of the FWS^{4}P with fifteen PENG strips in grip practicing, dumbbell curling and cycling. The fifteen PENG strips were connected in parallel and divided into five groups, and each group of the triplicates were taped together layer by layer with double-sided tape. In the grip practice scenario, the PENG triplets were fixed on the middle finger joints (proximal interphalangeal joints) and the sweat sensor patch on the back of the forearm just below the wrist (Fig. 5a). The hand-muscle developer was squeezed twice per second, and the output current averaged 45.6 μA (Fig. 5b). In the dumbbell curling scenario, the PENG triplets were fixed side by side in the elbow pit (cubital fossa) crossing the elbow crease, and the sweat sensor patch was fixed on the ventral side of the wrist (Fig. 5c). A dumbbell of 2.5 Kg was lifted in standard dumbbell bicep curls at 1 Hz, resulting in an average output current of 45 μA (Fig. 5d). In the cycling scenario, the PENG triplets were fixed in the knee pit (popliteal fossa) crossing the knee crease, and the sweat sensor patch was fixed nearby on the back of the thigh (Fig. 5e). Pedaling speed was maintained at 1 cycle per second, which resulted in an average output current of 41.3 μA (Fig. 5f). Output voltage and transferred charge were measured in the arm and leg application scenarios; see Fig. S11 for details. As shown in Fig. 5g and j, after charging capacitor (5 *1000 μF) to 3.7 V, the sweat sensor system was turned on. After signal processing, the information is transmitted by Bluetooth module to a smart phone (Fig. 5i and j; see video).

Supplementary material related to this article can be found online at doi:10.1016/j.nanoen.2021.106786.

Five data points are collected during an experimenter keep riding for 150 min. The multipoint data collection is also a common used method for a long time sweat monitoring, which can reflect physiological information during a long-time exercise from energetic to tired (or dehydration) [58–63]. Besides, we also continuously monitored the ions in sweat with a battery for one-hour exercise, the data was collected every five minutes (see Fig. S12), which showed similar trend with PENG powered multipoint data collection with a long-term sampling interval in Fig. 5h. Three indicators (Na+, K+ and pH) are all in the normal physiological range (Fig. 5h). In general, based on different individuals and stimulation methods to collect sweat, the concentrations of Na^+, K^+ and pH in human sweat are 10–100 mM, 3–10 mM and 4.5–7, respectively [64–66]. These data could change slightly with the exercise intensity, measurement position, humid and diet. For example, some literature reported the concentration range of Na^+, K^+ and pH are 20.3–112.3 mM, 4.2–13.8 mM and 4–6.8, respectively [67,68]. In our on-body test, Na^+ concentration increased with exercise time, which can be attributed to the low fluid loss rate under the cover of sweat sensor patch. The low sweat secretion rate reduces dilution and increases accumulation of Na^+ in the collected sweat [69]. The overall trend of K^+ concentration slightly decrease and fluctuate around 7 mM, this variation is in agreement with that reported in literature [70,71], it can be attributed to the variation of exercise intensity of subject and sweat transfer rate in microchannel. The pH variation was related to the exercise intensity, the concentration of ammonia in sweat decrease when exercise because it changes into ammonium (NH_4^+). The exercise intensity of subject decreases with time because of physical strength loss, leading to the reduce of accumulated NH_4^+ concentration in sweat, and further resulting in the pH decrease [67]. These three physiological indicators are all within normal range during the exercise. On the other hand, in practical application, to make the data has statistical significance, more volunteers should be recruited and tested. Meanwhile, it is also necessary to set standard for a large sample size. Fig. 5j shows the working module during energy collection and management, circuit operation, signal process and transmission. PVDF served as the energy generation module. After rectification, the electricity was stored in capacitor with 5 * 1000 μF capacity. When its voltage reached to a threshold value, the electricity will be released to power the Bluetooth module and instrument amplifier, then transmit the processed signal to user interface.

3. Conclusion

In summary, this work presents a flexible and wearable piezoelectricity-based self-sustainable sweat sensor system that is completely powered by human joint movements. The power source PENG could be easily fixed on large or small joints (e.g., finger joint, elbow joint and knee joint), and shows ideal mechanical and electric stability while converting the biomechanical energy harvested from joint bending into electricity. The conformal property of the FWS^{4}P allows it to stay fixed on skin surface, effectively and automatically collecting sweat, while utilizing the piezoelectricity enabled by PENG and the joints in proximity to power its sweat composition analysis.

The Na^+, K^+ and pH ISEs in the sweat sensor patch show consistent, repeatable and stable performance across the spectrum of physiologically relevant conditions, and the resulted health information is transmitted to a user interface via the Bluetooth module built in the flexible integrated circuit. On the other hand, because PENG generates pulse electricity with joint bending, which has to be managed and stored first and then power the circuit and sweat sensor patch. Therefore, it takes some time before collecting data. To further improve the applicability, reduce exercise intensity, realize data collection within several minutes and even achieve continuous monitoring of sweat, we discussed the future development directions of PENG:

3.1. Improve electric output and energy conversion efficiency

Whether the PENGs serve as power source or active sensor in a self-sustainable system, energy density is a key parameter in determining

continuous and stable operation of the entire system. So, researchers should continually improve the output of PENGs. Developing new materials, designing innovative structures and integrating low-energy circuits will be an essential step to realize more practical applicability in wireless sensor networks. For example, increasing specific surface area with micro/nano morphology, doping with chemical elements and surface modification, these treatment help to achieve a higher power density and enhance the sensitivity of PENG as active sensors. Additionally, it is also suggested to prepare composite materials by mixing inorganic piezoelectric materials with organic polymer, which combined the high piezoelectric coefficient of inorganic materials and the good flexibility of organic polymers. This method is conducive to synthesizing flexible piezoelectric materials and utilizing both piezoelectric effects of inorganic materials and organic polymers to attain high output.

3.2. Integrate electronic elements into an all-in-one system

The ultimate aim of PENGs focuses on the practical application, therefore, massive efforts should be paid on integrated sensors with multiple functions and artificial intelligence by combining machine learning and remote control. Besides, integrating other electronic elements in self-powered system and achieving self-sustainable operation of the whole wireless sensor nodes will finally facilitate the PENG application as active sensors or power source in wireless sensor networks.

3.3. Durability

To convert mechanical energy into electricity, it is inevitable to generate repeated deformation in practical applications, which will influence the structures of material and device, and ultimately destroy the PENG, reduce its output performance and shorten the service life. A feasible solution is to package the PENG with robust polymer and enhance its stability and durability. The materials commonly used for package are PET (polyethylene terephthalate), PDMS (polydimethylsiloxane), PI (polyimide) and so on.

Finally, with more system level investigations, wherein PENGs are integrated with energy storage elements, control circuits, power conditioning circuits and sensors, this technology will be capable of serving as a promising self-sustainable and eco-friendly power source for future wearable electronics to wirelessly monitor individual healthcare in daily exercise.

4. Materials and methods

4.1. Materials

3,4-Ethylenedioxythiophene (EDOT), sodium polystyrene sulfonate (PSS), sodium ionophore X, valinomycin, bis(2-ethylehexyl) sebacate (DOS), Polyvinyl Butyral (PVB), polyvinyl chloride (PVC), sodium tetrakis [3,5-bis(trifluoromethyl)phenyl] borate (Na-TFPB), sodium tetraphenylboron (NaTPB), aniline, calcium chloride dihydrate ($CaCl_2.2\ H_2O$), block polymer PEO-PPO-PEO (F127), multiwall carbon nanotubes (MWCNTs), iron(III) chloride ($FeCl_3$), and citric acid were purchased from Macklin. Sodium chloride (NaCl), Potassium chloride (KCl), methanol, ethanol, acetone, tetrahydrofuran (THF), cyclohexanone, hydrochloric acid (HCl), tetrachloroauric acid ($HAuCl_4$), and disodium phosphate (Na_2HPO_4) were purchased from Aladdin. Ag/AgCl ink was purchased from Structure Probe Inc. (SPI) supplies. PI film (175 μm thick) was purchased from Sigma. PVDF was purchased from ZHIMK Technology (Shen Zhen) CO., Ltd. and used without further treatment. NMD-3 2.38% developer, PM-THINNER developer and SP-01 stripping buffer were purchased from Suzhou Research Semiconductor (Resemi) Co., Ltd.

4.2. Preparation of sensor patch with microfluidic structure

The detailed preparation technology is shown in Fig. S3. The sensor patch was first patterned on PI film using positive photoresist (AZ1500) and UV light, followed by sputtering Cr (thickness, 30 nm) and Au (thickness, 100 nm). The residual photoresist was lift-off in SP-01 stripping buffer. After that, a 2 μm insulation layer was fabricated by spin-coating negative photoresist (SU-8 2025) onto the sensor quad, and then patterned by photolithography and developed in developing liquid (PM-THINNER) to expose the electrodes. Finally, a 100 μm microchannel layer was fabricated by spin-coating negative photoresist (SU-8 2025); the channels were patterned by photolithography and developed in developing liquid (PM-THINNER).

4.3. Preparation of biosensors

The three sensors (Na^+ sensor, K^+ sensor and pH sensor) were on the one sweat sensor patch to detect each ions. The left and right are Na^+ sensor and pH sensor, respectively. The up and down are K^+ sensor and reference electrode, respectively. Working electrodes (Na^+ and K^+) have two layers, including PEDOT layer and ion selective membrane. To prepare PEDOT layer, Au electrodes were immersed in the mixed solution of 0.01 M EDOT and 0.1 M NaPSS. Then PEDOT layer was deposited on Au layer under the current of 200 μA for 100 s. PEDOT layer as ion-electron transducer can minimize the potential drift of ISEs and improve the electrode performance (see Fig. S13). To prepare Na^+ selective membrane, THF (660 μl) was used as solvent to dissolve Na-TFPB (0.55%, w/w), Na^+ ionophore X (1%, w/w), DOS (65.45%, w/w) and PVC (33%, w/w). Then 15 μl of solution was drop cast onto the PEDOT/Au electrode. To prepare K^+ selective membrane, cyclohexanone (350 μl) was used as solvent to dissolve the mixture (100 mg) of valinomycin (1%, w/w), NaTPB (0.55%, w/w), PVC (33%, w/w) and DOS (65.5%, w/w). Then 15 μl of solution was drop cast onto the PEDOT/Au electrodes. To prepare pH working electrode, Au electrode was immersed in the mixture solution of $HAuCl_4$ (50 mM) and HCl (50 mM), and electrochemically deposited at 0 V for 30 s. Then, immerse the Au electrode in the mixture of aniline (0.1 M) and HCl (0.1 M) and deposit for 50 cycles. Scan rate and range were 50 mV/s and −0.2 to 1 V, respectively. To prepare the reference electrode, we first printed Ag/AgCl ink onto the Au electrode. Then prepared the reference solution, which consisted of PVB (79.1 mg), NaCl (50 mg), F127 (1 mg) and MWCNT (0.2 mg) in methanol (1 ml). Finally, drop cast 20 μl of reference solution onto the Ag/AgCl electrode above. The solutions above were stored at 4 °C when not in use.

4.4. Characterization of biosensor performance

To make the sensors maintain the best performance, a maintenance solution containing 0.1 M Na^+ and 0.1 M K^+ was prepared to store the sensors. To test relevant performance, the sensors were immersed in NaCl solution from 10 mM to 200 mM, KCl solutions from 1 mM to 20 mM and Mcllvaine's buffers with pH values from 3–8, respectively. To verify the selectivity, solutions containing Na^+ (50 mM), K^+ (50 mM), and Ca^{2+} (50 mM) were added in turn into the reaction system. To verify the long-term stability, the sensors were tested for many times during one month.

4.5. Electric characterization of PENG

The short-circuit current and transferred charge were recorded using an electrometer (Keithley 6517B) and an oscilloscope (Teledyne LeCroy HDO6104).[72–75] The open-circuit voltage and charging curves were measured using an oscilloscope (Teledyne LeCroy HDO6104). The electric variation of voltage, current and transferred charges versus frequency were measured using a linear motor.

4.6. On-body sweat detection experiment

The on-body sweat detection experiment was performed by the author Tianrui Chang, and this experiment was approved by the institutional review board of China-Japan Friendship Hospital (2021–112-K70). The author was also informed and signed consent form before taking part in the experiment.

4.7. Preparation of PENG

The PENG has a layer by layer structure, including PET encapsulation layer as the supporting substrate, silver ink layer as the electrode of PVDF, and PVDF piezoelectric layer. Before encapsulate the PVDF with PET, PVDF was firstly coated with silver ink to cover its surface, after dried in air, the PVDF film was poled at 100 ℃ and applied a direct electric field of 100 kV/cm for 20 h [76]. Then cut the poled PVDF film into proper shape and size, and encapsulate it with PET film using hot-press. Finally, connect electrodes to the reserved silver ink using conductive fixture (see Fig. S14). The key step is the high voltage polarization of PVDF, if without the treatment, PVDF has few ability to convert mechanical energy into electricity. Meanwhile, PET encapsulation can protect the PENG from damage during repeated bending.

CRediT authorship contribution statement

Hu Li and Lingqian Chang conceived the ideas and designed the experiments. Hu Li, Tianrui Chang developed the PENG, sweat sensor, and measured their performance. Tianrui Chang and Yansong Gai measured the performance of PENG. Kui Liang fabricated the flexible circuit. Yanli Jiao, Dengfeng Li, Xinran Jiang and Yang Wang improved the draft writing. Xingcan Huang, Han Wu and Yiming Liu assisted in fabricating the sweat sensor and microfluidic channel. Jian Li, Yiming Bai and Kai Geng assisted in developing the flexible circuit. Nianrong Zhang and Hua Meng assisted in on-body sweat test and ethical evaluation. Dongsheng Huang, Zhou Li, Xinge Yu and Lingqian Chang supervised this project.

Declaration of Competing Interest

The authors declare that they have no known competing financial interests or personal relationships that could have appeared to influence the work reported in this paper.

Acknowledgements

This work was supported by the Beijing Advanced Innovation Center for Biomedical Engineering, National Natural Science Foundation of China (Grant No. 32071407, 62003203, T2125003 and 61875015), Beijing Natural Science Foundation (No. 7212204), City University of Hong Kong (Grants No. 9610423, 9667199, 9667221, 9680322), Research Grants Council of the Hong Kong Special Administrative Region (Grant No. 21210820, 11213721), Shenzhen Science and Technology Innovation Commission (Grant No. JCYJ20200109110201713).

Appendix A. Supporting information

Supplementary data associated with this article can be found in the online version at doi:10.1016/j.nanoen.2021.106786.

References

[1] M. Bariya, H.Y.Y. Nyein, A. Javey, Wearable sweat sensors, Nat. Electron. 1 (2018) 160–171.
[2] W. He, C. Wang, H. Wang, M. Jian, W. Lu, X. Liang, X. Zhang, F. Yang, Y. Zhang, Integrated textile sensor patch forreal-time and multiplex sweat analysis, Sci. Adv. 5 (2019) eaax0649.
[3] Z. Sonner, E. Wilder, J. Heikenfeld, G. Kasting, F. Beyette, D. Swaile, F. Sherman, J. Joyce, J. Hagen, N. KelleyLoughnane, R. Naik, The microfluidics of the eccrine sweat gland, including biomarker partitioning, transport, and biosensing implications, Biomicrofluidics 9 (2015), 031301.
[4] H. Li, S. Gu, Q. Zhang, E. Song, T. Kuang, F. Chen, X. Yu, L. Chang, Recent advances in biofluid detection with micro/nanostructured bioelectronic devices, Nanoscale 13 (2021) 3436–3453.
[5] Y. Yang, W. Gao, Wearable and flexible electronics for continuous molecular monitoring, Chem. Soc. Rev. 48 (2019) 1465–1491.
[6] Z. Sonner, E. Wilder, T. Gaillard, G. Kasting, J. Heikenfeld, Integrated sudomotor axon reflex sweat stimulation for continuous sweat analyte analysis with individuals at rest, Lab Chip 17 (2017) 2550–2560.
[7] A.J. Bandodkar, J. Wang, Non-invasive wearable electrochemical sensors: a review, Trends Biotechnol. 32 (2014) 363–371.
[8] J. Tu, R.M. Torrente-Rodríguez, M. Wang, W. Gao, The era of digital health: a review of portable and wearable affinity biosensors, Adv. Funct. Mater. 30 (2020), 1906713.
[9] J. Kim, A.S. Campbell, B. Esteban-Fernández de Ávila, J. Wang, Wearable biosensors for healthcare monitoring, Nat. Biotechnol. 37 (2019) 389–406.
[10] T.R. Ray, J. Choi, A.J. Bandodkar, S. Krishnan, P. Gutruf, L. Tian, R. Ghaffari, J. A. Rogers, Bio-integrated wearable systems: a comprehensive review, Chem. Rev. 119 (2019) 5461–5533.
[11] Y. Khan, A.E. Ostfeld, C.M. Lochner, A. Pierre, A.C. Arias, Monitoring of vital signs with flexible and wearable medical devices, Adv. Mater. 28 (2016) 4373–4395.
[12] Z. Rao, Y. Lu, Z. Li, K. Sim, Z. Ma, J. Xiao, C. Yu, Curvy, shape-adaptive imagers based on printed optoelectronic pixels with a kirigami design, Nat. Electron. 4 (2021) 513–521.
[13] X. Yu, Z. Xie, Y. Yu, J. Lee, A. Vazquez-Guardado, H. Luan, J. Ruban, X. Ning, A. Akhtar, D. Li, B. Ji, Y. Liu, R. Sun, J. Cao, Q. Huo, Y. Zhong, C. Lee, S. Kim, P. Gutruf, C. Zhang, Y. Xue, Q. Guo, A. Chempakasseril, P. Tian, W. Lu, J. Jeong, Y. Yu, J. Cornman, C. Tan, B. Kim, K. Lee, X. Feng, Y. Huang, J.A. Rogers, Skin-integrated wireless haptic interfaces for virtual and augmented reality, Nature 575 (2019) 473–479.
[14] E. Song, Z. Xie, W. Bai, H. Luan, B. Ji, X. Ning, Y. Xia, J.M. Baek, Y. Lee, R. Avila, H.-Y. Chen, J.-H. Kim, S. Madhvapathy, K. Yao, D. Li, J. Zhou, M. Han, S.M. Won, X. Zhang, D.J. Myers, Y. Mei, X. Guo, S. Xu, J.-K. Chang, X. Yu, Y. Huang, J. A. Rogers, Miniaturized electromechanical devices for the characterization of the biomechanics of deep tissue, Nat. Biomed. Eng. 5 (2021) 759–771.
[15] T. Kaya, G. Liu, J. Ho, K. Yelamarthi, K. Miller, J. Edwards, A. Stannard, Wearable sweat sensors: background and current trends, Electroanal 31 (2019) 411–421.
[16] A.M. Zamarayeva, A.E. Ostfeld, M. Wang, J.K. Duey, I. Deckman, B.P. Lechêne, G. Davies, D.A. Steingart, A.C. Arias, Flexible and stretchable power sources for wearable electronics, Sci. Adv. 3 (2017), e1602051.
[17] J. Li, J. Zhao, J.A. Rogers, Materials and designs for power supply systems in skin-interfaced electronics, Acc. Chem. Res. 52 (2018) 53–62.
[18] S. Park, S.W. Heo, W. Lee, D. Inoue, Z. Jiang, K. Yu, H. Jinno, D. Hashizume, M. Sekino, T. Yokota, K. Fukuda, K. Tajima, T. Someya, Self-powered ultra-flexible electronics via nano-grating-patterned organic photovoltaics, Nature 561 (2018) 516–521.
[19] L. Yin, J.-M. Moon, J.R. Sempionatto, M. Lin, M. Cao, A. Trifonov, F. Zhang, Z. Lou, J.-M. Jeong, S.-J. Lee, S. Xu, J. Wang, A passive perspiration biofuel cell: High energy return on investment, Joule 5 (2021) 1888–1904.
[20] H.S. Wang, S.K. Hong, J.H. Han, Y.H. Jung, H.K. Jeong, T.H. Im, C.K. Jeong, B.-Y. Lee, G. Kim, C.D. Yoo, K.J. Lee, Biomimetic and flexible piezoelectric mobile acoustic sensors with multiresonant ultrathin structures for machine learning biometrics, Sci. Adv. 7 (2021) eabe5683.
[21] R. Hinchet, H.-J. Yoon, H. Ryu, M.-K. Kim, E.-K. Choi, D.-S. Kim, S.-W. Kim, Transcutaneous ultrasound energy harvesting using capacitive triboelectric technology, Science 365 (2019) 491–494.
[22] Y. Zou, V. Raveendran, J. Chen, Wearable triboelectric nanogenerators for biomechanical energy harvesting, Nano Energy 77 (2020), 105303.
[23] W. Xu, H. Zheng, Y. Liu, X. Zhou, C. Zhang, Y. Song, X. Deng, M. Leung, Z. Yang, R. X. Xu, Z.L. Wang, X.C. Zeng, Z. Wang, A droplet-based electricity generator with high instantaneous power density, Nature 578 (2020) 392–396.
[24] W. He, W. Liu, J. Chen, Z. Wang, Y. Liu, X. Pu, H. Yang, Q. Tang, H. Yang, H. Guo, C. Hu, Boosting output performance of sliding mode triboelectric nanogenerator by charge space-accumulation effect, Nat. Commun. 11 (2020) 1–8.
[25] Y. Shi, F. Wang, J. Tian, S. Li, E. Fu, J. Nie, R. Lei, Y. Ding, X. Chen, Z.L. Wang, Self-powered electro-tactile system for virtual tactile experiences, Sci. Adv. 7 (2021) eabe2943.
[26] X. Zhao, Z. Zhang, Q. Liao, X. Xun, F. Gao, L. Xu, Z. Kang, Y. Zhang, Self-powered user-interactive electronic skin for programmable touch operation platform, Sci. Adv. 6 (2020) eaba4294.
[27] M. Zhu, Z. Sun, T. Chen, C. Lee, Low cost exoskeleton manipulator using bidirectional triboelectric sensors enhanced multiple degree of freedom sensory system, Nat. Commun. 12 (2021) 1–16.
[28] X. Zhao, H. Askari, J. Chen, Nanogenerators for smart cities in the era of 5G and Internet of Things, Joule 5 (2021) 1391–1431.
[29] Z.L. Wang, J. Song, Piezoelectric nanogenerators based on zinc oxide nanowire arrays, Science 312 (2006) 242–246.
[30] F. Yang, J. Li, Y. Long, Z. Zhang, L. Wang, J. Sui, Y. Dong, Y. Wang, R. Taylor, D. Ni, W. Cai, P. Wang, T. Hacker, X. Wang, Wafer-scale heterostructured piezoelectric bio-organic thin films, Science 373 (2021) 337–342.
[31] L. Lu, W. Ding, J. Liu, B. Yang, Flexible PVDF based piezoelectric nanogenerators, Nano Energy 78 (2020), 105251.

[32] L. Gu, J. Liu, N. Cui, Q. Xu, T. Du, L. Zhang, Z. Wang, C. Long, Y. Qin, Enhancing the current density of a piezoelectric nanogenerator using a three-dimensional intercalation electrode, Nat. Commun. 11 (2020) 1–9.
[33] Y.H. Jung, S.K. Hong, H.S. Wang, J.H. Han, T.X. Pham, H. Park, J. Kim, S. Kang, C. D. Yoo, K.J. Lee, Flexible piezoelectric acoustic sensors and machine learning for speech processing, Adv. Mater. 32 (2020), 1904020.
[34] D.W. Lee, D.G. Jeong, J.H. Kim, H.S. Kim, G. Murillo, G.-H. Lee, H.-C. Song, J. H. Jung, Polarization-controlled PVDF-based hybrid nanogenerator for an effective vibrational energy harvesting from human foot, Nano Energy 76 (2020), 105066.
[35] H.E. Lee, J. Choi, S.H. Lee, M. Jeong, J.H. Shin, D.J. Joe, D. Kim, C.W. Kim, J.H. Park, J.H. L, D. Kim, C.-S. Shin, K.J. Lee, Monolithic flexible vertical GaN light-emitting diodes for a transparent wireless brain optical stimulator, Adv. Mater. 30 (2018) 1800649.
[36] B.H. Mun, B.K. You, S.R. Yang, H.G. Yoo, J.M. Kim, W.I. Park, Y. Yin, M. Byun, Y. S. Jung, K.J. Lee, Flexible one diode-one phase change memory array enabled by block copolymer self-assembly, ACS Nano 9 (2015) 4120–4128.
[37] S.L. Zhang, M. Xu, C. Zhang, Y.-C. Wang, H. Zou, X. He, Z. Wang, Z.L. Wang, Rationally designed sea snake structure based triboelectric nanogenerators for effectively and efficiently harvesting ocean wave energy with minimized water screening effect, Nano Energy 48 (2018) 421–429.
[38] C. Zhang, L. He, L. Zhou, O. Yang, W. Yuan, X. Wei, Y. Liu, L. Lu, J. Wang, Z. L. Wang, Active resonance triboelectric nanogenerator for harvesting omnidirectional water-wave energy, Joule 5 (2021) 1613–1623.
[39] Y. Zou, P. Tan, B. Shi, H. Ouyang, D. Jiang, Z. Liu, H. Li, M. Yu, C. Wang, X. Qu, L. Zhao, Y. Fan, Z.L. Wang, Z. Li, A bionic stretchable nanogenerator for underwater sensing and energy harvesting, Nat. Commun. 10 (2019) 1–10.
[40] K. Parida, G. Thangavel, G. Cai, X. Zhou, S. Park, J. Xiong, P.S. Lee, Extremely stretchable and self-healing conductor based on thermoplastic elastomer for all-three-dimensional printed triboelectric nanogenerator, Nat. Commun. 10 (2019) 1–9.
[41] F. Fan, W. Tang, Z.L. Wang, Flexible nanogenerators for energy harvesting and self-powered electronics, Adv. Mater. 28 (2016) 4283–4305.
[42] J. Briscoe, S. Dunn, Piezoelectric nanogenerators: a review of nanostructured piezoelectric energy harvesters, Nano Energy 14 (2015) 15–29.
[43] G.-T. Hwang, H. Park, J.-H. Lee, S. Oh, K.-I. Park, M. Byun, H. Park, G. Ahn, C. K. Jeong, K. No, H. Kwon, S.-G. Lee, B. Joung, K.J. Lee, Self-powered cardiac pacemaker enabled by flexible single crystalline PMN-PT piezoelectric energy harvester, Adv. Mater. 26 (2014) 4880–4887.
[44] X. Cheng, X. Xue, Y. Ma, M. Han, W. Zhang, Z. Xu, H. Zhang, H. Zhang, Implantable and self-powered blood pressure monitoring based on a piezoelectric thin film: simulated, in vitro and in vivo studies, Nano Energy 22 (2016) 453–460.
[45] D.H. Kim, H.J. Shin, H. Lee, C.K. Jeong, H. Park, G.-T. Hwang, H.-Y. Lee, D.J. Joe, J.H. Han, S.H. Lee, J. Kim, B. Joung, K.J. Lee, In vivo self-powered wireless transmission using biocompatible flexible energy harvesters, Adv. Funct. Mater. 27 (2017), 1700341.
[46] D.Y. Park, D.J. Joe, D.H. Kim, H. Park, J.H. Han, C.K. Jeong, H. Park, J.G. Park, B. Joung, K.J. Lee, Self-powered real-time arterial pulse monitoring using ultrathin epidermal piezoelectric sensors, Adv. Mater. 29 (2017), 1702308.
[47] G.-T. Hwang, Y. Kim, J.-H. Lee, S. Oh, C.K. Jeong, D.Y. Park, J. Ryu, H. Kwon, S.-G. Lee, B. Joung, D. Kim, K.J. Lee, Self-powered deep brain stimulation via a flexible PIMNT energy harvester, Energy Environ. Sci. 8 (2015) 2677–2684.
[48] P. Wan, X. Wen, C. Sun, B.K. Chandran, H. Zhang, X. Sun, X. Chen, Flexible transparent films based on nanocomposite networks of polyaniline and carbon nanotubes for high-performance gas sensing, Small 11 (2015) 5409–5415.
[49] S. Yang, Y. Liu, W. Chen, W. Jin, J. Zhou, H. Zhang, G.S. Zakharova, High sensitivity and good selectivity of ultralong MoO_3 nanobelts for trimethylamine gas, Sens. Actuators B 226 (2016) 478–485.
[50] J. Liu, X. Jiang, R. Zhang, Y. Zhang, L. Wu, W. Lu, J. Li, Y. Li, H. Zhang, MXene-enabled electrochemical microfluidic biosensor: applications toward multicomponent continuous monitoring in whole blood, Adv. Funct. Mater. 29 (2019), 1807326.
[51] D. Tyagi, H. Wang, W. Huang, L. Hu, Y. Tang, Z. Guo, Z. Ouyang, H. Zhang, Recent advances in two-dimensional-material-based sensing technology toward health and environmental monitoring applications, Nanoscale 12 (2020) 3535.
[52] Z. Liu, L. Xu, Q. Zheng, Y. Kang, B. Shi, D. Jiang, H. Li, X. Qu, Y. Fan, Z.L. Wang, Z. Li, Human motion driven self-powered photodynamic system for long-term autonomous cancer therapy, ACS Nano 14 (2020) 8074–8083.
[53] H. Yu, J. Sun, Sweat detection theory and fluid driven methods: a review, Nanotechnol. Precis. Eng. 3 (2020) 126–140.
[54] B. Zhong, K. Jiang, L. Wang, G. Shen, Wearable sweat loss measuring devices: from the role of sweat loss to advanced mechanisms and designs, Adv. Sci. (2021), 2103257.
[55] J. Choi, D. Kang, S. Han, S.B. Kim, J.A. Rogers, Thin, soft, skin-mounted microfluidic networks with capillary bursting valves for chrono-sampling of sweat, Adv. Healthc. Mater. 6 (2017), 1601355.
[56] A. Martín, J. Kim, J.F. Kurniawan, J.R. Sempionatto, J.R. Moreto, G. Tang, A. S. Campbell, A. Shin, M.Y. Lee, X. Liu, J. Wang, Epidermal microfluidic electrochemical detection system: enhanced sweat sampling and metabolite detection, ACS, Sensors 2 (2017) 1860–1868.
[57] R. Ghaffari, D.S. Yang, J. Kim, A. Mansour, J.A. Wright, J.B. Model Jr., D.E. Wright, J.A. Rogers, T.R. Ray, State of sweat: emerging wearable systems for real-time, noninvasive sweat sensing and analytics, ACS Sens. 6 (2021) 2787–2801.
[58] Y. Yang, Y. Song, X. Bo, J. Min, O.S. Pak, L. Zhu, M. Wang, J. Tu, A. Kogan, H. Zhang, T.K. Hsiai, Z. Li, W. Gao, A laser-engraved wearable sensor for sensitive detection of uric acid and tyrosine in sweat, Nat. Biotechnol. 38 (2020) 217–224.
[59] S.Y. Oh, S.Y. Hong, Y.R. Jeong, J. Yun, H. Park, S.W. Jin, G. Lee, J.H. Oh, H. Lee, S.-S. Lee, J.S. Ha, ACS Appl. Mater. Interfaces 10 (2018) 13729–13740.
[60] P.T. Toi, T.Q. Trung, T.M.L. Dang, C.W. Bae, N.-E. Lee, Highly electrocatalytic, durable, and stretchable nanohybrid fiber for on-body sweat glucose detection, ACS Appl. Mater. Interfaces 11 (2019) 10707–10717.
[61] A.P. Selvam, S. Muthukumar, V. Kamakoti, S. Prasad, A wearable biochemical sensor for monitoring alcohol consumption lifestyle through Ethyl glucuronide (EtG) detection in human sweat, Sci. Rep. 6 (2016) 23111.
[62] R.A. Oppliger, C. Bartok, Hydration testing of athletes, Sports Med 32 (2002) 959–971.
[63] D.L. Costill, R. Cote, W. Fink, Muscle water and electrolytes following varied levels of dehydration in man, J. Appl. Physiol. 40 (1976) 6–11.
[64] P. Pirovano, M. Dorrian, A. Shinde, A. Donohoe, A.J. Brady, N.M. Moyna, G. Wallace, D. Diamond, M. McCaul, A wearable sensor for the detection of sodium and potassium in human sweat during exercise, Talanta 219 (2020), 121145.
[65] F. Herrmann, L. Mandol, Studies of pH of sweat produced by different forms of stimulation, J. Invest. Dermatol. 24 (1955) 225–246.
[66] S.J. Montain, S.N. Cheuvront, H.C. Lukaski, Sweat mineral-element responses during 7h of exercise-heat stress, Int. J. Sport Nutr. Exerc. Metab. 17 (2007) 574–582.
[67] W. Dang, L. Manjakkal, W.T. Navaraj, L. Lorenzelli, V. Vinciguerra, R. Dahiya, Stretchable wireless system for sweat pH monitoring, Biosens. Bioelectron. 107 (2018) 192–202.
[68] S.R. Corrie, J.W. Coffey, J. Islam, K.A. Markey, M.A.F. Kendall, Blood, sweat, and tears: developing clinically relevant protein biosensors for integrated body fluid analysis, Analyst 140 (2015) 4350–4364.
[69] R. Vinoth, T. Nakagawa, J. Mathiyarasu, A.M.V. Mohan, Fully printed wearable microfluidic devices for high-throughput sweat sampling and multiplexed electrochemical analysis, ACS Sens. 6 (2021) 1174–1186.
[70] P. Pirovano, M. Dorrian, A. Shinde, A. Donohoe, A.J. Brady, N.M. Moyna, G. Wallace, D. Diamond, M. McCaul, A wearable sensor for the detection of sodium and potassium in human sweat during exercise, Talanta 219 (2020), 121145.
[71] M. Parrilla, I. Ortiz-Gomez, R. Canovas, A. Salinas-Castillo, M. Cuartero, G. A. Crespo, Wearable potentiometric ion patch for on-body electrolyte monitoring in sweat: toward a validation strategy to ensure physiological relevance, Anal. Chem. 91 (2019) 8644–8651.
[72] H. Li, L. Zhao, J. Meng, C. Pan, Y. Zhang, Y. Zhang, Z. Liu, Y. Zou, Y. Fan, Z. L. Wang, Z. Li, Triboelectric-polarization-enhanced high sensitive ZnO UV sensor, Nano Today 33 (2020), 100873.
[73] H. Li, X. Zhang, L. Zhao, D. Jiang, L. Xu, Z. Liu, Y. Wu, K. Hu, M.-R. Zhang, J. Wang, Y. Fan, Z. Li, A hybrid biofuel and triboelectric nanogenerator for bioenergy harvesting, Nano-Micro Lett. 12 (2020) 1–12.
[74] P. Bertani, W. Lu, Cyanobacterial toxin biosensors for environmental monitoring and protection, Med. Nov. Technol. Devices 10 (2021), 100059.
[75] H. Li, H. Ouyang, M. Yu, N. Wu, X. Wang, W. Jiang, Z. Liu, J. Tian, Y. Jin, H. Feng, Y. Fan, Z. Li, Thermo-driven evaporation self-assembly and dynamic analysis of homocentric carbon nanotube rings, Small 13 (2017), 1603642.
[76] S.-H. Shin, Y.-H. Kim, M.H. Lee, J.-Y. Jung, J. Nah, Hemispherically aggregated $BaTiO_3$ nanoparticle composite thin film for high-performance flexible piezoelectric nanogenerator, ACS Nano 8 (2014) 2766.

Hu Li is a Postdoctoral Fellow at the Department of Biomedical Engineering, City University of Hong Kong, Hong Kong, China. He received his Ph.D. from Beihang University, China, in 2020, and his Bachelor's degree from Tianjin Polytechnic University, China, in 2014. His research interests are focused on nanogenerators, self-powered sensors, flexible electronics and bioelectronics.

Tianrui Chang is currently a master student at School of Biological Science and Medical Engineering, Beihang University, China. He obtained his Bachelor's Degree in Biomedical Engineering from Northeastern University, China. His research interests include wearable and flexible sensor and MEMS fabrication.

Yansong Gai is currently pursuing a Ph.D. degree in School of Chemistry and Chemical Engineering at the Guangxi University. His research interests are mainly focused on nanogenerators, flexible electronics and bioelectronics, and self-powered systems.

Kui Liang received the M.S. degree in Chemistry from China University of Geosciences, Beijing, China. Since 2011, he has been as a Researcher with the BOE Technology Group Co., Ltd., Beijing, China, where he is involved in Flexible Electronics. His research interests include E-Skin, Flexible sensor, soft actuators and new material.

Yanli Jiao is currently a Ph.D. Student in the College of Engineering / Department of Biomedical Engineering at the City University of Hong Kong. She obtained her master in Food Process Engineering from the Illinois Institute of Technology. Her research is mainly focused on biosensor and analytical chemistry.

Dengfeng Li is currently a Postdoctoral Fellow in department of Biomedical Engineering, City University of Hong Kong. He received the Bachelor degree from Xi'an Jiaotong University, Master degree from Tsinghua University, and the Ph.D. degree from City University of Hong Kong. His research interests include flexible electronics, skin-integrated haptic interface for VR/AR, and soft robotics.

Xinran Jiang is currently a research assistant in the School of Biological Science and Medical Engineering at Beihang University. She obtained her M.S. degree at Weill Cornell Graduate School of Medical Sciences and her B.S. degree at University of Washington. Her research background includes signaling pathways in different types of cells (e.g., monocytes/macrophages, dermal fibroblasts, endothelial cells), and the role of exosomes in cancer metastases.

Yang Wang is currently an associate professor in the School of Engineering Medicine at the Beihang University. He did post-doctoral research in the School of Mechanical Engineering at the University of Minnesota, Twin Cities. He obtained his Ph.D. and M.S. degrees in Bioelectronics from Institute of Electronics, Chinese Academy of Sciences. His reaches mainly include microfluidic devices, point-of-care testing methods and MEMS techniques.

Xingcan Huang received his Master degree in 2020 from Shandong University, and he obtained his B.S. degree in 2017 from Qingdao University. Now, he is pursuing his Ph.D. degree in City University of Hong Kong. His current research interests focus on flexible biosensors, flexible biomedical devices, and flexible battery.

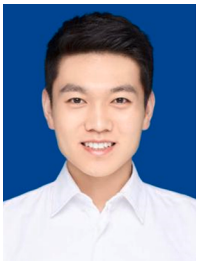

Han Wu is currently a Ph.D. student at the School of Biological and Medical Engineering, Beihang University. He obtained a master's degree in industrial catalysis and a bachelor's degree in applied chemistry from Xi'an University of Science and Technology, China. His research mainly focuses on the research and development of microbial nanochips, which can be implanted in vivo flexible micro and nanochips.

Yiming Liu received his M.Sc. in 2017 from The Hong Kong University of Science and Technology, and he obtained his bachelor degree in Tianjin University in China in 2015. Now he is pursuing his Ph.D. degree in City University of Hong Kong. His current research interests focus on flexible self-powered electronics, human machine interfaces, and flexible battery.

Jian Li received the M.S. degree in Material Science from Tianjin University,Beijing, China. since 2012. He has been as a Researcher with the BOE Technology Group Co., Ltd., Beijing, China. His reresearch is mainly focused on flexible sensor, such as sensor materials and preparation process technology.

Yiming Bai received the Ph.D. degree in microelectronics from TSINGHUA University, Beijing, China. Since 2016, he has been as a PM with the BOE Technology Group Co., Ltd., Beijing, China, where he is involved in IC technology. His research interests include clock generation, frequency synthesis, hardware security and instruction set architecture.

Kai Geng received the M.S. degree in Instrument Science and Technology from Tianjin University, China. since 2019. He has been as a Researcher with the BOE Technology Group Co., Ltd., Beijing, China. His reresearch is mainly focused on software development, such as mobile applications and computer software development.

Nianrong Zhang is currently a resident in General Surgery Department & Obesity and Metabolic Disease Center at China-Japan Friendship Hospital. She obtained her Ph.D. in Medical from Peking Union Medical College. Her research interests include the pathogenesis and prognostic factors of diabetic nephropathy.

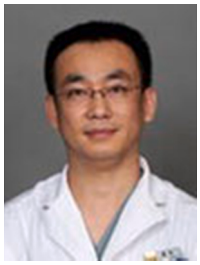

Hua Meng is currently the Director of General Surgery Department & Obesity and Metabolic Disease Center at China-Japan Friendship Hospital and he is also a doctoral supervisor at Capital Medical University, China. He obtained his Ph.D. in Medical from Zhejiang University, China. He has been engaged in the diagnosis and treatment of gastrointestinal diseases for a long time, and is good at laparoscopic treatment of gastrointestinal diseases.

Dongsheng Huang received the M.S. degree in Polymer Chemistry and Physics from NanKai University, China. Since 2005. He has been as a researcher with the BOE Technology Group Co., Ltd., Beijing, China, where he is involved in sensor device and system. His research interests include flexible sensor, sensor materials and preparation process technology.

Prof. Zhou Li received his Bachelor's degree from Wuhan University in 2004, and Doctor's Degree from Peking University in Department of Biomedical Engineering in 2010. He joined School of Biological Science and Medical Engineering of Beihang University in 2010 as an associate Professor. Currently, he is principal investigator and group leader of Nanoenergy and Biosystem Lab (NBL) in Beijing Institute of Nanoenergy and Nanosystems, Chinese Academy of Sciences. His research interests include nanogenerators, in vivo energy harvesters and self-powered medical devices, biosensors.

Prof. Xinge Yu is currently an Assistant Professor of Biomedical Engineering at City University of Hong Kong. He got bachelor degree from University of electronics Science and Technology of China in 2009 and received his Ph.D. degree in Optical Engineering from UESTC in 2015. Now Xinge Yu's research group is focusing on skin-integrated electronics and systems for biomedical applications. He has published over 100 papers in the top journals, such as Nature, Nature Materials, Nature Biomedical Engineering, Nature Communications, PNAS, Science Advances etc., and held 20 patents pending or granted.

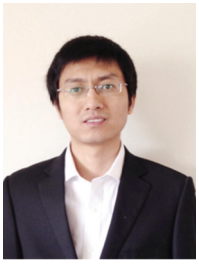

Prof. Lingqian Chang obtained his Ph.D. in Biomedical Engineering from Ohio State University, followed by postdoc training in CCNE nanoscale center at Northwestern University. He used to be an assistant professor at the University of North Texas. Currently he is a full professor at Beihang University, and founded The Institute of Single Cell Engineering. His research is mainly focused on cellular micro-/nano-technologies, aiming to design novel nanochips and nanosensors for gene detection and cell therapy in live cells. He has published more than 50 peer-reviewed papers, 1 book, 3 book chapters and hold 5 China Patents and 3 US Patents.